Journal of Organometallic Chemistry 768 (2014) 151–156

Contents lists available at ScienceDirect

Journal of Organometallic Chemistry

journal homepage: www.elsevier.com/locate/jorganchem

DFT study and dynamic NMR evidence for *cis-trans* conformational isomerism in square planar Ni(II) thioselenophosphinate, $Ni(SeSPPh_2)_2$

Alexander V. Artem'ev [a], Vladimir A. Shagun [a], Nina K. Gusarova [a], C.W. Liu [b], **, Jian-Hong Liao [b], Yurii V. Gatilov [c], [d], Boris A. Trofimov [a], *

[a] *A. E. Favorsky Irkutsk Institute of Chemistry, Siberian Branch of the Russian Academy of Sciences, 1 Favorsky Str., 664033 Irkutsk, Russian Federation*
[b] *Department of Chemistry, National Dong Hwa University, Hualien, Taiwan 97401, Republic of China*
[c] *N. N. Vorozhtsov Novosibirsk Institute of Organic Chemistry, Siberian Branch of the Russian Academy of Sciences, 9 Lavrentiev Ave., 630090 Novosibirsk, Russian Federation*
[d] *Novosibirsk State University, 2 Pirogova Str., Novosibirsk 630090, Russian Federation*

ARTICLE INFO

Article history:
Received 1 March 2014
Received in revised form
21 May 2014
Accepted 16 June 2014
Available online 8 July 2014

Keywords:
Nickel
DFT calculations
VT ^{31}P NMR
Spin-crossover
Thioselenophosphinate

ABSTRACT

Theoretical (DFT) and experimental (dynamic NMR) study of *cis-trans* conformational isomerism in Ni(II) square planar thioselenophosphinate, $Ni(SeSPPh_2)_2$, have been carried out. The DFT investigation [B3LYP/6-311++G(d,p), gas] of this complex reveals that its *cis-to-trans* isomerization occurs through two minimal energy crossing points (MECPs) located at the intersection of the lowest singlet and triplet PESs (potential energy surfaces). The calculated relative energies of the MECPs, 5.6 and 3.6 kcal/mol, correspond to low-energy barriers of "*cis*-$Ni(SeSPPh_2)_2$ [S] $\rightleftharpoons$ *pseudoterahedral*-$Ni(SeSPPh_2)_2$ [T]" and "*trans*-$Ni(SeSPPh_2)_2$ [S] $\rightleftharpoons$ *pseudoterahedral*-$Ni(SeSPPh_2)_2$ [T]" spin crossover rearrangements. The dynamic ^{31}P NMR study of $Ni(SeSPPh_2)_2$ is fully confirms these computations: below 208 K, the *cis*- and *trans*-isomers are in a dynamic equilibrium. The free energy of activation for this fluxional process calculated from the coalescence temperature is $\Delta G^{\neq} = 11.5$ kcal/mol.

Introduction

Metal dichalcogenophosphinates represent an important class of organophosphorus compounds that are widely used both in industry and academic research [1]. Among them, the most significant are metal dithiophosphinates, which are frequently applied as intermediate forms in selective liquid–liquid extraction of metal ions [2] as well as flotation reagents [3]. Less attention has been paid to the diselenophosphinates [4] and, especially, thioselenophosphinates [5], however, their chemistry is developing rapidly. Coordination chemistry of dichalcogenophosphinates has a distinctive structural diversity due to their abilities to form unique molecular structures (mono-, bi-, tetra-, hexa-, octa-, etc.) [1,4,6], many of which are effective single-source precursors to semiconductive metal selenides nanocrystals [7].

Obviously, structural information such as calculations of geometrical and electronic configurations, molecular dynamics as well as thermodynamic and magnetic properties of the dichalcogenophosphinato complexes is an important basis for understanding the different factors influencing their practically useful properties. For example, structural investigations of metal dichalcogenophosphinates can provide insight into the complex processes occurring at the liquid–liquid extraction of metals as well as can be helpful for the design of more selective extractants for metal separation, e.g. Ln^{III} and An^{III} [8]. In this field, there are series of works devoted to DFT and *ab initio* computations of metal dithiophosphinates (lanthanides and actinides [9], Co and Ni [10], Au [11], Na [12]) and, in a less degree, diselenophosphinates (Ce, Nd, Th, Pa, U, Np, Pu) [13].

More recently, developing the chemistry of thioselenophosphinic acids, we have identified an interesting structural feature for the solid state structure of Ni(II) thioselenophosphinates, $Ni(SeSPR_2)_2$, (R = Ph or CH_2CH_2Ph) [5a]. Namely, the chalcogen atoms of square planar $Ni(SeS)_2$ unit, according to X-ray diffraction analysis, are disordered over the two positions. For this reason, it is unclear what isomer (*cis*-, *trans*- or

---

* Corresponding author. Tel.: +7 395242 14 11; fax: +7 395241 93 46.
** Corresponding author. Tel.: +86 886 3 8633607; fax: +86 886 3 8633570.
E-mail addresses: chenwei@mail.ndhu.edu.tw (C.W. Liu), boris_trofimov@irioch.irk.ru (B.A. Trofimov).

http://dx.doi.org/10.1016/j.jorganchem.2014.06.013
0022-328X/© 2014 Elsevier B.V. All rights reserved.

their mixture) forms the crystal packing? Furthermore, the $Ni(SeSPR_2)_2$ complexes are expected to undergo interconversion in solution state. Indeed, it is known that the chelate complexes $M(A\hat{}B)_2$ where A^B are flexible bidentate ligands can adopt different conformations, which are often in a dynamic exchange [14]. In particular, for square planar Ni(II) complexes, an inversion of the A^B ligands through a tetrahedral intermediate is specific (spin-crossover equilibrium) [14d,15], which should lead to a conformational isomerism of *cis-trans* type (Scheme 1). Moreover, in solution these isomers can be detected by NMR spectroscopy, if the rate of the exchange is appropriate for NMR time scale [15,16]. At the same time, in the literature, to our surprise, there are no data on existence of the *cis-trans* isomerism for square planar Ni(II) complexes bearing thiophosph(in)ate $[O(S)PR_2]$ ligands, not to mention selenophosph(in)ates $[O(Se)PR_2]$, thioselenophosph(in)ates $[S(Se)PR_2]$ or related ligands (thiocarboxylates, selenocarboxylates and thioselenocarboxylates).

In continuation of our research into selenophosph(in)ato metal complexes, we have investigated the possibility of *cis-trans* conformational isomerization within Ni(II) thioselenophosphinato complex $[Ni(SeSPPh_2)_2]$. Accordingly, the main questions addressed in this work are (*i*) to provide insight into detailed mechanism of this process using DFT calculations and, (*ii*) to verify experimentally (by dynamic ^{31}P NMR spectroscopy) the equilibrium between two isomeric forms. Concurrently, herein we report an original one-pot method for the synthesis of these complexes and crystal structure of one from them.

Results and discussion

One-pot synthesis of complexes **2a–c**

Usually, transition metal thioselenophosphinates are prepared by ion exchange between alkali metal [17] or ammonium thioselenophosphinates [18] and metal salts. We have elaborated facile and efficient one-pot synthesis of Ni(II) thioselenophosphinates from available [19] secondary phosphines **1a–c** (Scheme 2). So, the latter are treated with powdered selenium in benzene solution (35–40 °C, 30 min) to give secondary phosphine selenides $R_2P(Se)H$, which further react (without isolation) with S_8/NaOH system (stoichiometric ratio, ethanol, 23–25 °C, 5 min) to provide sodium thiselenophosphinates. Finally, $NiCl_2$ is added to the resulting thioselenophosphinates to afford the target complexes **2a–c** in 69–81% yields.

Complexes **2a–c** have been characterized by solution ^1H, ^{31}P, ^{77}Se NMR spectroscopy. The elemental analyses of the compounds support their compositions. The complexes **2a**,**b** were characterized previously by X-ray crystallography [5a], while the structure of earlier unknown complex **2c** was determined for the first time. The crystals of **2c** contain discrete monomeric molecules (Fig. 1), exhibiting square planar $Ni(SSe)_2$ cores, in which the Ni(II) ion is chelated by two sulfur and two selenium atoms in the equatorial plane (deviations from the mean plane being ± 0.056 Å). Thus, the both thioselenophosphinate anions act as S,Se-bidentane (η^2) ligands. The selenium and sulfur atoms are disordered over two positions in 0.716(1):0.284(1) ratio with the retention of *cis* atomic arrangement of selenium. The bond lengths of Ni–S and Ni–Se are consistent with those in square planar complexes **2a**,**b** [5a] and tetrahedral complex $Ni[^iPr_2P(S)NP(Se)^iPr_2]_2$ [20], in which S and Se atoms are also disordered. Within the extended structure of **2c**, between neighboring molecules there are weak intermolecular C(8)-H … Se(2) [2.82 Å, 148°] and π(O4CCCC) … π(O4CCCC) [Cg … Cg 3.609(2), d_{pl} 3.505 Å] interactions.

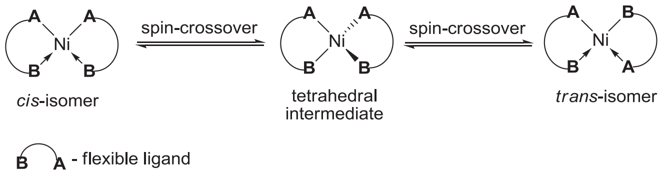

Scheme 1. *Cis-to-trans* conformational isomerization for square planar $Ni(A\hat{}B)_2$ complexes proceeding *via* spin-crossover equilibrium.

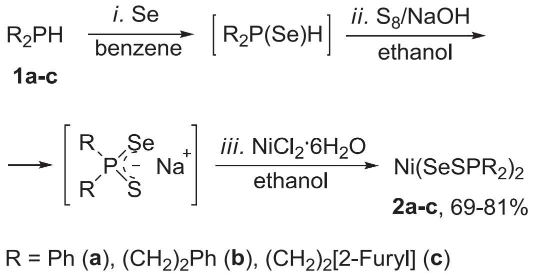

Scheme 2. One-pot synthesis of complexes **2a–c**. Conditions: *i.* 35–40 °C, 30 min; *ii.* 23–25 °C, 5 min; *iii.* 23–25 °C, 5 min.

Theoretical study

Obviously, *cis-to-trans* rearrangement of diamagnetic ($S = 0$) square-planar $Ni(SeSPPh_2)_2$ complex occurs *via* pseudotetrahedral paramagnetic ($S = 1$) forms **A**, Scheme 3. It was shown earlier [14d,21], that the diagonal twist mechanism of rotation rearrangement within bis-chelate complexes is more energetically favorable than the bond rupture-formation pathway. Taking this into consideration, we have constructed B3LYP/6-311++G(d,p) energy profile of the rotation isomerization of model complex $Ni(SeSPPh_2)_2$ (**2a**) for singlet and triplet states along the *exo*-Se-Ni-S twisting angle (*β*, deg). For this purpose, methods developed by Harvey [22] for the study of mechanisms associated with the spin-state changing are applied. This approach is based on the determination of minimum energy crossing points (MECPs) on the seam of intersecting lowest singlet and triplet PESs. Recently, this procedure has been successfully employed to establish the spin-forbidden isomerization pathways for several bis-chelate Ni(II) complexes [23].

The energy profiles for the conformational isomerization of **2a** as the function of the twisting angle *β* are shown in Fig. 2. The value of this angle within *trans*-isomer is taken as the starting point

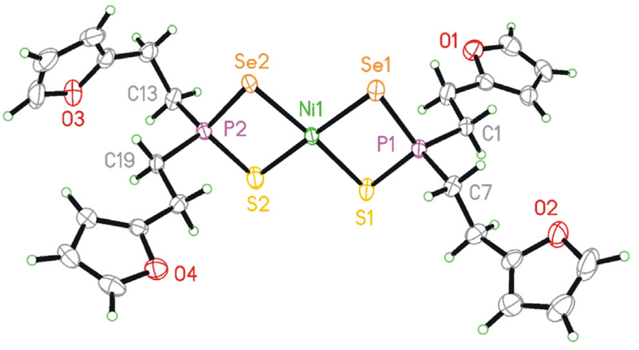

Fig. 1. Molecular structure of **2c** with 50% probability ellipsoids (minor disorder S and Se atoms omitted for clarity). Selected bond lengths (Å) and bond angles (deg): Ni(1)-Se(1) 2.3666(6), Ni(1)-Se(2) 2.3487(6), Ni(1)-S(1) 2.2990(7), Ni(1)-S(2) 2.2741(8), P–Se 2.1462(9), 2.1503(9), P–S 2.106(1), 2.088(1), P–C 1.809(3) – 1.819(3), Se(1)-Ni(1)-Se(2) 91.56(2), S(1)-Ni(1)-S(2) 86.99(3), S(1)-Ni(1)-Se(1) 91.25(2), S(2)-Ni(1)-Se(2) 90.28(2).

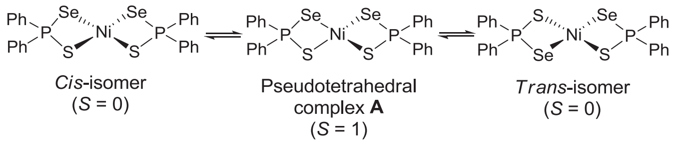

Scheme 3. A tentative pathway for interconversion of square-planar complex **2a**.

(β = 0). The structures corresponding to the stationary points appeared on the singlet (S) and triplet (T) PESs are pictured in Fig. 3, while the energy data related to for key structures are collected in Table 1.

On the singlet PES there are two minima corresponding to *cis*- and *trans*-square-planar isomers, *cis*-**2a** and *trans*-**2a**, having a minor difference in energy. The *trans*-isomer is found to be slightly stable than the *cis*-isomer by 0.3 kcal/mol. On the triplet PES, the complex **2a** is stabilized in a pseudotetrahedral conformation, *pseudotetrahedral*-**2a** (T), the relative energy of which is 1.1 kcal/mol (Table 1, Fig. 2).

In the singlet state, *trans-to-cis* rearrangement [*trans*-**2a**(S) → *cis*-**2a**(S)] is associated with overcoming the activation barrier in the 25.6 kcal/mol. The structure of the corresponding transition state, **TS1**, is depicted in Fig. 2. The rotation isomerization of the pseudotetrahedral structure on the triplet PES could potentially occurs through the two channels, i.e. either *via* planar state having *cis*-oriented chalcogen atoms (**TS2**) or state with *trans*-disposed S and Se atoms (**TS3**). The first pathway is attributed to with overcoming the activation barrier in the 5.4 kcal/mol, while the second channel requires overcoming the barrier in 2.7 kcal/mol (Figs. 2 and 3, Table 1).

The existence of two non-generative stationary states on the singlet PES leads to formation of two multidimensional seams of crossing between the singlet and the triplet PESs. The intersection of the two curves occurs at the **A1** and **A2** regions, where the change of the spin state (crossover) for *cis*-**2a** and *trans*-**2a** complexes takes place. The minimal energy reaction paths including the spin-crossover are shown in Fig. 2 as double lines passed through **A1** and **A2** regions. To find the MECPs, the geometries of structures located at the **A1** and **A2** regions are taken as the initial guesses. The optimizations of these structures are performed until the energy differences for the singlet and triplet states do not exceed 0.00003 and 0.000005 a.u. for **MECP1** and **MECP2**, respectively. The values of the dihedral angle β within **MECP1** and **MECP2** structures are 162 and 19° (Fig. 3).

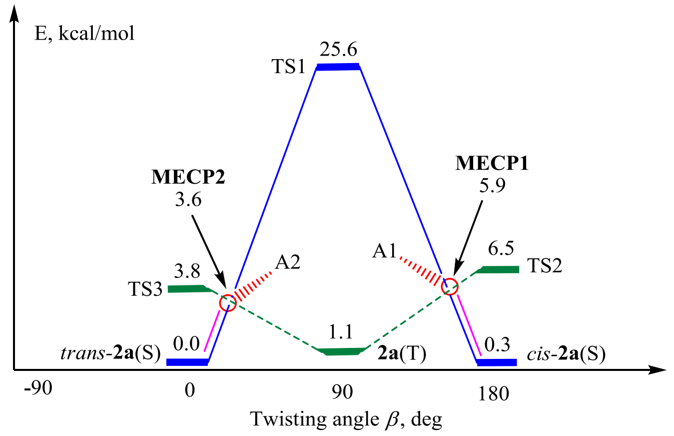

Fig. 2. Energy profile for the *trans* ⇌ *cis* stereoisomerization of $Ni(SeSPPh_2)_2$ (**2a**) shown as the functions of the *exo*-S-Ni-Se twisting angle (β, deg). The solid line for the singlet PES; dashed line for the triplet PES; double solid for the spin forbidden reactions.

The gradient descent from the **MECP1** along the singlet and triplet PESs leads to two minima which correspond to *cis*-**2a**(S) and *pseudotetrahedral*-**2a**(T) structures (Fig. 2). The similar procedure performed for **MECP2** leads to *trans*-**2a**(S) and *pseudotetrahedral*-**2a**(T) structures.

Thus, the calculated relative energies of the **MECP1** and **MECP2** (5.6 and 3.6 kcal/mol) represent the activation barriers for "*cis*-**2a** ⇌ *pseudoterahedral*-**2a**" and "*trans*-**2a** ⇌ *pseudoterahedral*-**2a**" stereoisomerizations, respectively. Simplistically, *cis-to-trans* isomerization of $Ni(SeSPPh_2)_2$ is associated with overcoming of two activation barriers, 5.6 and 2.5 kcal/mol. Considering these values, we have concluded that the conformational isomerization of $Ni(SeSPPh_2)_2$ complexes is rather probable process.

*VT ^{31}P NMR study of complex **2a***

To verify the predicted *cis-trans* interconversion for Ni(II) thioselenophosphinates, we have undertaken VT ^{31}P NMR study of the complexes **2a** in CD_2Cl_2 solution over the temperature range from −90 to 18 °C. At ambient temperature ^1H NMR spectrum of **2a** reveals characteristic peaks corresponding to organic groups of the ligands. The ^{31}P NMR spectrum shows a slightly broad peak at 56.44 ppm flanked by a pair of blurry satellites due to the $^{31}P-^{77}Se$ splitting (Fig. 4). Upon cooling of the solution, the peak becomes broad and maximum of broadening is at −65 °C (coalescence temperature). At −80 °C, new broad peaks emerge at 58.81 and 60.11 ppm (in integral ratio of ~1:1) along with small medial peak at 58.42 ppm, which is caused by overlapping of ^{77}Se satellites from major peaks. On further decreasing the temperature to −90 °C, the spectrum of **2a** contains two signals (59.08 and 60.48 ppm) as well as minor peak (59.75 ppm) from the overlapping ^{77}Se satellites. These results indicate that the fluxional process within complex **2a** slows down upon lowering the temperature.

This observation is clearly indicates on predicted interconversion between *cis*- and *trans*-isomers of complex **2a**. The ^{31}P NMR chemical shifts of the individual isomers are different below −80 °C, however, at higher temperatures, when the exchange rate is high, a single averaged signal is observed. Using the Gutowski-Holm approximation $k_c = \pi^*\Delta\nu/\sqrt{2}$(where $\Delta\nu$ is difference between the ^{31}P chemical shift of two peaks) [24], the rate constant, k_c, for the equilibrium process is calculated. The free energy of activation, calculated based on Eyring equation $\Delta G^{\neq} = RT_c[\ln T_c - \ln k_c + 23.76]$ [24,25] (where T_c is coalescence temperature, i.e. 208 K), is *ca.* 11.5 kcal mol^{-1}. This value is quite comparable with the predicted one: a discrepancy is caused by influence of the solvent.

Conclusions

To summary, by using DFT computations combined with dynamic NMR spectroscopy, we have clearly established the *cis-trans* conformational isomerism for square planar complex $Ni(SeSPPh_2)_2$. It has been computed that the *cis-to-trans* isomerization of $Ni(SeSPPh_2)_2$ proceeds *via* triplet pseudotetrahedral intermediate. This transition is associated with overcoming of two minimal activation barriers, 5.6 and 2.5 kcal/mol, which energetically correspond to **MECP1** and **MECP2** states on intersecting singlet and triplet PESs. The predicted phenomenon is fully confirmed by dynamic ^{31}P NMR spectroscopy, i.e. *cis*- and *trans*-isomers of the complexes **2a** are presented in solution below 208 K. At higher temperature, the rate of the *cis-trans* interconversion is faster than the NMR time scale, so the both isomers appear to be identical. The data obtained are essential complement to the coordination and inorganic chemistry.

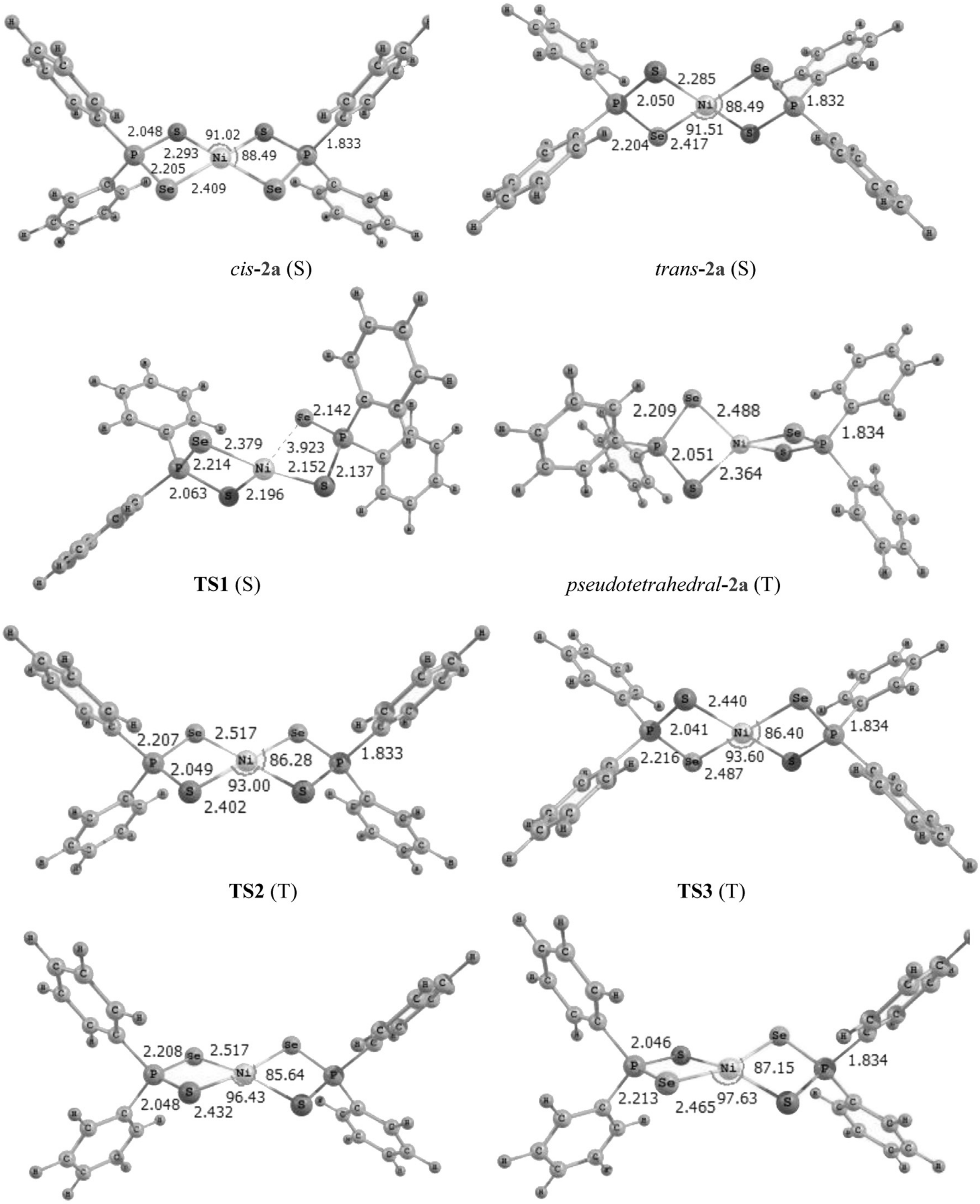

cis-**2a** (S)

trans-**2a** (S)

TS1 (S)

pseudotetrahedral-**2a** (T)

TS2 (T)

TS3 (T)

MECP1

MECP2

Fig. 3. Optimized structures and selected metrics for key states of Ni(SeSPPh$_2$)$_2$ (**2a**) stereoisomerization calculated by B3LYP/6-311++G(d,p) method (bond lengths and angles are given in Å and degrees).

Experimental

Computational details

The DFT calculations were carried out in Gaussian 09 package [26] using the B3LYP functional [27] and 6-311++G(d,p) basis set. Minimum energy structures were found by steepest descent path (gradient line) optimization from transition states or from the MECP to a neighboring stationary point. Harmonic vibrational frequencies were calculated at the same level of theory to identify all stationary points. Transition states were located on the PESs using quadratic synchronous transit (QST) method [28]. All calculations were performed for isolated molecules.

*One-pot synthesis of complexes **2a**–**c***

To a solution of freshly distilled secondary phosphine **1a**–**c** (1 mmol) in benzene (12 mL), powdered selenium (79 mg, 1 mmol) was added and the mixture was stirred at 35–40 °C until the dissolution of Se (*ca*. 30 min). In this solution, powdered sulfur S$_8$

Table 1
Total energies (E_{tot}), total energies with the account for zero point energy ($E_{tot\,+\,ZPE}$) and relative energies (ΔE and $\Delta E_{tot\,+\,ZPE}$), for key states of Ni(SeSPPh$_2$)$_2$ (**2a**) stereo-isomerization calculated by B3LYP/6-311++G(d,p) method.

Structure	Multiplicity	E_{tot} (a.u.)	ΔE (Kcal/mol)	$E_{tot\,+\,ZPE}$ (a.u.)	$\Delta E_{tot\,+\,ZPE}$ (Kcal/mol)
cis-**2a**	S	8717.618927	0.3	8717.245909	0.3
trans-**2a**	S	8717.619329	0.0	8717.246368	0.0
pseudotetrahedral-**2a**	T	8717.617610	1.1	8717.244651	1.1
TS1	S	8717.578526	25.6	8717.205819	25.4
TS2	T	8717.608959	6.5	8717.236599	6.2
TS3	T	8717.613271	3.8	8717.240309	3.8
MECP1		8717.609981	5.9		
MECP2		8717.613556	3.6		

(32 mg, 0.125 mmol) was dissolved and solution of NaOH (40 mg, 1.0 mmol) in EtOH (3 mL) was added to the prepared mixture at stirring (23–25 °C, 5 min). To a resulting solution of sodium thioselenophosphinate, NiCl$_2$·6H$_2$O (119 mg, 0.5 mmol) in EtOH (10 mL) was added. The mixture was stirred for 5 min at 23–25 °C, diluted with water (30 mL) and extracted with CH$_2$Cl$_2$ (1 × 20 mL). The organic layer was washed with water (2 × 10 mL), dried over Na$_2$SO$_4$ and evaporated in vacuum. The solid obtained was dissolved in CH$_2$Cl$_2$ (5 mL) and the solution was layered with hexane (20 mL) to afford complexes **2a**–**c**.

*Characterization data for complexes **2a**–**c***

*Nickel(II) diphenylthioselenophosphinate (**2a**)*

Dark-green crystals, mp 223–225 °C (CH$_2$Cl$_2$/hexane). Yield: 240 mg (74%). Anal. Calcd for C$_{24}$H$_{20}$NiP$_2$S$_2$Se$_2$ (651.11): C, 44.27; H, 3.10. Found: C, 44.20; H, 3.15. ^{1}H NMR (400.13 MHz, CDCl$_3$): δ = 7.46–7.55 (m, 12H, Ph), 7.76–7.82 (m, 8H, Ph). ^{31}P NMR (161.98 MHz, CDCl$_3$): δ = 56.44. The ^{77}Se NMR spectrum of **2a** was unavailable due to the poor solubility.

*Nickel(II) bis(2-phenethyl)thioselenophosphinate (**2b**)*

Dark-green crystals, mp 133–140 °C (CH$_2$Cl$_2$/hexane). Yield: 310 mg (81%). Anal. Calcd for C$_{32}$H$_{36}$NiP$_2$S$_2$Se$_2$ (763.32): C, 50.35; H, 4.75. Found: C, 50.24; H, 4.91. ^{1}H NMR (400.13 MHz, CDCl$_3$): δ = 2.29–2.36 (m, 8H, CH$_2$P), 3.22–3.29 (m, 8H, CH$_2$Ph), 7.23–7.34 (m, 20H, Ph). ^{31}P NMR (161.98 MHz, CDCl$_3$): δ = 73.73 (s, $^1J_{PSe}$ = 458 Hz). ^{77}Se NMR (76.31 MHz, CDCl$_3$): δ = −346 (d, $^1J_{PSe}$ = 458 Hz).

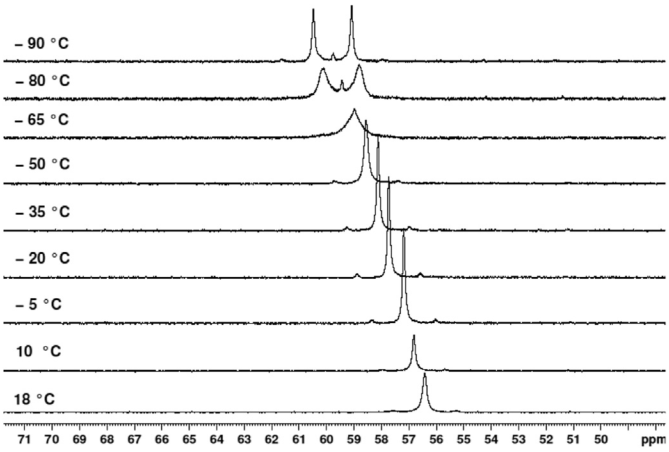

Fig. 4. VT ^{31}P NMR spectra of complex **2a** in CD$_2$Cl$_2$ solution.

*Nickel(II) bis(2-furan-2-ylethyl)thioselenophosphinate (**2c**)*

Dark-green crystals, dec. > 130 °C (CH$_2$Cl$_2$/hexane). Yield: 250 mg (69%). Anal. Calcd for C$_{24}$H$_{28}$NiO$_4$P$_2$S$_2$Se$_2$ (723.17): C, 39.86; H, 3.90. Found: C, 39.71; H, 4.02. ^{1}H NMR (400.13 MHz, CDCl$_3$): δ = 2.18–2.27 (m, 8H, CH$_2$P), 2.80–2.90 (m, 8H, CH$_2$Fur), 6.03–7.29 (m, 12H, Fur). ^{31}P NMR (161.98 MHz, CDCl$_3$): δ = 72.05 (s, $^1J_{PSe}$ = 450 Hz). ^{77}Se NMR (76.31 MHz, CDCl$_3$): δ = −340 (d, $^1J_{PSe}$ = 450 Hz).

X-ray crystallography

The X-ray quality single crystals of **2c** were obtained by layering of its CH$_2$Cl$_2$ solutions with hexane at room temperature. Data were collected using the ω scans on a Bruker Kappa Apex II CCD diffractometer with graphite monochromated Mo-K$_\alpha$ radiation with λ = 0.71073 Å, and corrected for absorption using the multi-scan method. The structure was solved using Patterson Methods, followed by a Tangent Expansion (ShelXS). Non-hydrogen atoms were refined anisotropically using SHELXTL97 [29]. Hydrogen atoms were included at geometrically calculated positions during the refinement using the riding model. The restrictions (equality of parameters for atoms of one position) were used with the refinement, in the other variants the refinement led to the poorer results.

Crystal data for **2c**: C$_{24}$H$_{28}$NiO$_4$P$_2$S$_2$Se$_2$, M_r = 723.15, triclinic, space group *P*-1, a = 8.7352(6) Å, b = 11.5844(8) Å, c = 15.0548(11) Å, α = 71.764(2)°, β = 81.602(3)°, γ = 78.834(2)°, V = 1413.54(17) Å^3, Z = 2, d_{calc} = 1.699 g/cm^{-3}, μ(Mo-K$_\alpha$) = 3.551 mm^{-1}, θ_{max} = 30.0°, measured/independent reflections 22,946/7879 (R_{int} = 0.0335), data/restraints/parameters: 7879/0/318, R indices: R_1 = 0.0376 [5080 $I > 2\sigma(I)$], wR_2 (all data) = 0.1293, GOF on F^2 = 1.012.

Acknowledgments

This work was supported by the President of the Russian Federation (program for the support of leading scientific schools, grant NSh-156.2014.3). The authors are also grateful to Victor I. Mamatyuk for performing VT ^{31}P NMR study of complex **2a**.

Appendix A. Supplementary material

CCDC 855044 contains the supplementary crystallographic data for this paper. These data can be obtained free of charge from The Cambridge Crystallographic Data Centre *via* www.ccdc.cam.ac.uk/data_request/cif.

Appendix B. Supplementary data

Supplementary data related to this article can be found at http://dx.doi.org/10.1016/j.jorganchem.2014.06.013.

References

[1] (a) C. Silvestru, I. Haiduc, Coord. Chem. Rev. 147 (1996) 117;
(b) I. Haiduc, Coord. Chem. Rev. 158 (1997) 325;
(c) H.P.S. Chauhan, Coord. Chem. Rev. 173 (1998) 1;
(d) F. Nief, Coord. Chem. Rev. 180 (1998) 13;
(e) I. Haiduc, J. Organomet. Chem. 623 (2001) 29;
(f) I. Haiduc, L.Y. Goh, Coord. Chem. Rev. 224 (2002) 151;
(g) W.E. Van Zyl, Comments Inorg. Chem. 31 (2010) 13.

[2] (a) Y. Zhu, J. Chen, R. Jiao, Solvent Extr. Ion. Exch. 14 (1996) 61;
(b) D.R. Peterman, M.R. Greenhalgh, R.D. Tillotson, J.R. Klaehn, M.K. Harrup, T.A. Luther, J.D. Law, Sep. Sci. Technol. 45 (2010) 1711;
(c) F. Wang, C. Jia, D. Pan, Ji Chen, Ind. Eng. Chem. Res. 52 (2013) 18373.

[3] (a) E.T. Pecina-Treviño, A. Uribe-Salas, F. Nava-Alonso, R. Pérez-Garibay, Inter. J. Min. Proc. 71 (2003) 201;
(b) T. Güler, C. Hiçyilmaz, G. Gökagaç, Z. Ekmeçi, Min. Eng. 19 (2006) 62;
(c) V.A. Chanturia, T.A. Ivanova, E.V. Koporulina, J. Min. Sci. 45 (2009) 164.

[4] (a) T.S. Lobana, J.-C. Wang, C.W. Liu, Coord. Chem. Rev. 251 (2007) 91;
(b) A.V. Artem'ev, N.K. Gusarova, S.F. Malysheva, B.A. Trofimov, Org. Prep. Proc. Int. 43 (2011) 381.

[5] (a) A.V. Artem'ev, N.K. Gusarova, I.Yu Bagryanskaya, E.P. Doronina, S.I. Verkhoturova, V.F. Sidorkin, B.A. Trofimov, Eur. J. Inorg. Chem. (2013) 415;
(b) A.C. Behrle, C.L. Barnes, N. Kaltsoyannis, J.R. Walensky, Inorg. Chem. 52 (2013) 10623.

[6] (a) I. Haiduc, D.B. Sowerby, Polyhedron 15 (1995) 2469;
(b) I. Haiduc, in: J.A. McCleverty, T.J. Meyer (Eds.), Comprehensive Coordination Chemistry II, Elsevier Oxford, 2003, pp. 349–376;
(c) J.D. Woollins, R.S. Laitinen, Selenium and Tellurium Chemistry: from Small Molecules to Biomolecules and Materials, Springer, Berlin, 2011.

[7] (a) A. Panneerselvam, C.Q. Nguyen, J. Waters, M.A. Malik, P. O'Brien, J. Raftery, M. Helliwell, Dalton Trans. (2008) 4499;
(b) S.N. Malik, S. Mahboob, N. Haider, M.A. Malik, P. O'Brien, Nanoscale 3 (2011) 5132;
(c) W. Maneeprakorn, M.A. Malik, P. O'Brien, J. Mater. Chem. 20 (2010) 2329;
(d) M.P. Hendricks, B.M. Cossairt, J.S. Owen, ACS Nano 6 (2012) 10054.

[8] J.-H. Lan, W.-Q. Shi, L.-Y. Yuan, J. Li, Y.-L. Zhao, Z.-F. Chai, Coord. Chem. Rev. 256 (2012) 1406.

[9] (a) M.P. Jensen, A.H. Bond, J. Am. Chem. Soc. 124 (2002) 9870;
(b) C. Boehme, G. Wipff, Inorg. Chem. 38 (1999) 5734;
(c) A. Bhattacharyya, T.K. Ghanty, P.K. Mohapatra, V.K. Manchanda, Inorg. Chem. 50 (2011) 3913;
(d) C. Boehme, G. Wipff, Chem. Eur. J. 7 (2001) 1398;
(e) X. Cao, D. Heidelberg, J. Ciupka, M. Dolg, Inorg. Chem. 49 (2010) 10307;
(f) A.M. Mkadmh, A.A.S. Elkhaldy, A.M. Abu-Shanab, R.Y. Morjan, M.A. Elarag, J. Coord. Chem. 66 (2013) 1016.

[10] (a) A. Otero-Calvi, G. Aullon, S. Alvarez, L.A. Montero, W.-D. Stohrer, J. Mol. Struct. Theochem 767 (2006) 37;
(b) L.N. Mazalov, N.A. Kryuchkova, G.K. Parygina, O.A. Tarasenko, S.V. Trubina, J. Struct. Chem. 49 (19 (Supplement)) (2008);
(c) A. Otero-Calvi, L.A. Montero, W.-D. Stohrer, J. Mol. Struct. Theochem 859 (2008) 93;
(d) S.R. Daly, J.M. Keith, E.R. Batista, K.S. Boland, S.A. Kozimor, R.L. Martin, B.L. Scott, Inorg. Chem. 51 (2012) 7551.

[11] Y.-Q. Jiao, G.-W. Lu, K. Zhao, Y. Chen, J.-H. Lan, C.-J. Shao, Wang, J. Mol. Struct. Theochem 957 (2010) 1.

[12] C.M. Leavitt, G.L. Gresham, M.T. Benson, J.-J. Gaumet, D.R. Peterman, J.R. Klaehn, M. Moser, F. Aubriet, M.J. Van Stipdonk, G.S. Groenewold, Inorg. Chem. 47 (2008) 3056.

[13] M.B. Jones, A.J. Gaunt, J.C. Gordon, N. Kaltsoyannis, M.P. Neu, B.L. Scott, Chem. Sci. 4 (2013) 1189.

[14] (a) J.H. Nelson, D.A. Redfield, J. Am. Chem. Soc. 96 (1974) 6219;
(b) D.A. Redfield, J.H. Nelson, R.A. Henry, D.W. Moore, H.B. Jonassen, J. Am. Chem. Soc. 96 (1974) 6298;
(c) G. Alibrandi, L.M. Scolaro, R. Romeo, Inorg. Chem. 30 (1991) 4007;
(d) V.I. Minkin, L.E. Nivorozhkin, M.S. Korobov, Russ. Chem. Rev. 63 (1994) 289;
(e) Y.J. Kim, J.I. Park, S.C. Lee, K. Osakada, M. Tanabe, J.C. Choi, T. Koizumi, T. Yamamoto, Organometallics 18 (1999) 1349.

[15] (a) G.W. Everett Jr., R.H. Holm, J. Am. Chem. Soc. 87 (1965) 2117;
(b) G.W. Everett Jr., R.H. Holm, Inorg. Chem. 7 (1968) 776;
(c) R. Knoch, H. Elias, H. Paulus, Inorg. Chem. 34 (1995) 4032.

[16] (a) R. Knorr, A. Weiss, H. Polzer, E. Raepple, J. Am. Chem. Soc. 99 (1977) 650;
(b) Y.-P. Huang, C.-C. Tsai, W.-C. Shih, Y.-C. Chang, S.-T. Lin, G.P.A. Yap, I. Chao, T.-G. Ong, Organometallics 28 (2009) 4316.

[17] (a) H. Hertel, W. Kuchen, Chem. Ber. 104 (1971) 1735;
(b) H. Hertel, W. Kuchen, Chem. Ber. 104 (1971) 1740;
(c) P. Christophliemk, V.V.K. Rao, I. Tossidis, A. Muller, Chem. Ber. 105 (1972) 1736;
(d) A. Mueller, V.V.K. Rao, P. Christophliemk, J. Inorg. Nucl. Chem. 34 (1972) 345.

[18] J. Akhtar, M. Afzaal, M.A. Vincent, N.A. Burton, J. Raftery, I.H. Hillier, P. O'Brien, J. Phys. Chem. C 115 (2011) 16904.

[19] (a) B.A. Trofimov, N.K. Gusarova, Mendeleev Commun. 19 (2009) 295;
(b) N.K. Gusarova, S.N. Arbuzova, B.A. Trofimov, Pure Appl. Chem. 84 (2012) 439.

[20] A. Panneerselvam, M.A. Malik, M. Afzaal, P. O'Brien, M. Helliwell, J. Am. Chem. Soc. 130 (2008) 2420.

[21] (a) V.I. Minkin, V.A. Pichko, I.A. Abubikerova, B.Ya Simkin, J. Mol. Struct. Theochem 227 (1991) 295;
(b) J.M.H. Lo, M. Klobukowski, Inorg. Chim. Acta 353 (2003) 15.

[22] (a) J.N. Harvey, M. Aschi, H. Schwarz, W. Koch, Theor. Chem. Acc. 99 (1998) 95;
(b) R. Poli, J.N. Harvey, Chem. Soc. Rev. 32 (2003) 1.

[23] (a) A.G. Starikov, R.M. Minyaev, V.I. Minkin Chem, Phys. Lett. 459 (2008) 27;
(b) A.G. Starikov, R.M. Minyaev, V.I. Minkin, Russ. J. Gen. Chem. 79 (2009) 1793;
(c) A.G. Starikov, R.M. Minyaev, V.I. Minkin, J. Mol. Struct. Theochem 895 (2009) 138.

[24] M. Oki, Application of Dynamic NMR Spectroscopy to Organic Chemistry, Wiley, New York, 1985.

[25] H. Gunther, NMR Spectroscopy, second ed., Wiley, New York, 1995 (Chapter 9).

[26] M.J. Frisch, et al., Gaussian 09, Revision A01, Gaussian, Inc., Wallingford, 2009.

[27] A.D. Becke, J. Chem. Phys. 98 (1993) 5648.

[28] C. Peng, P.Y. Ayala, H.B. Schlegal, M.J. Frisch, J. Comp. Chem. 17 (1996) 49.

[29] Bruker Version 6.22, Bruker AXS Inc, Madison, WI, USA, 2003.